

A measurement of the τ lepton lifetime

JADE-Collaboration

C. Kleinwort², J. Allison⁵, K. Ambrus^{3,g}, R.J. Barlow⁵, W. Bartel¹, S. Bethke^{3,a}, C.K. Bowdery⁴, S.L. Cartwright^{7,b}, J. Chrin⁵, D. Clarke⁷, A. Dieckmann³, I.P. Duerdoth⁵, G. Eckerlin³, E. Elsen³, R. Felst¹, A.J. Finch⁴, F. Foster⁴, T. Greenshaw², J. Hagemann², D. Haidt¹, J. Heintze³, G. Heinzelmann², K.H. Hellenbrand^{3,c}, P. Hill^{6,h}, G. Hughes⁴, H. Kado^{1,i}, K. Kawagoe⁸, G. Knies¹, S. Komamiya^{3,c}, H. Krehbiel¹, J.v. Krogh³, M. Kuhlen^{2,j}, F.K. Loebinger⁵, A.A. Macbeth⁵, N. Magnussen^{1,d}, R. Marshall⁷, T. Mashimo⁸, R. Meinke¹, R.P. Middleton⁷, P.G. Murphy⁵, B. Naroska¹, J.M. Nye⁴, J. Olsson¹, F. Ould-Saada², R. Ramcke^{2,h}, H. Rieseberg³, D. Schmidt^{1,d}, H.v.d. Schmidt³, L. Smolik³, U. Schneekloth^{2,b}, J.A.J. Skard^{6,f}, J. Spitzer^{3,k}, P. Steffen¹, K. Stephens⁵, H. Takeda⁸, A. Wagner³, I.W. Walker⁴, G. Weber², M. Zimmer³, G.T. Zorn⁶

¹ Deutsches Elektronen-Synchrotron DESY, Hamburg, Federal Republic of Germany

² II. Institut für Experimentalphysik der Universität Hamburg, Hamburg, Federal Republic of Germany

³ Physikalisches Institut der Universität Heidelberg, Heidelberg, Federal Republic of Germany

⁴ University of Lancaster, Lancaster, England

⁵ University of Manchester, Manchester, England

⁶ University of Maryland, College Park, Md, USA

⁷ Rutherford Appleton Laboratory, Chilton, Didcot, England

⁸ International Center for Elementary Particle Physics, University of Tokyo, Tokyo, Japan

Received 7 November 1988

Abstract. The lifetime of the τ lepton was measured using two different techniques. From the impact parameter distribution of 3132 one prong decays $\tau_\tau = (289 \pm 33 \pm 26)$ fs was obtained and from the decay length distribution of 648 three prong decays $\tau_\tau = \left(309^{+35}_{-34} \pm 11 \right)$ fs. These results were combined to give a final value of $\tau_\tau = (301 \pm 29)$ fs.

parameter. A measurement of τ_τ enables for instance a test of lepton universality via the relationship

$$\tau_\tau = \tau_\mu (G_\mu/G_\tau)^2 (m_\mu/m_\tau)^5 B(\tau \rightarrow e \bar{\nu}_e \nu_\tau), \quad (1)$$

where $B(\tau \rightarrow e \bar{\nu}_e \nu_\tau)$ is the electronic τ branching fraction and $G_{\mu,\tau}$ the Fermi constant determined from μ and τ decay respectively. This article describes a measurement of τ_τ performed with the JADE-detector at the e^+e^- -storage ring PETRA.

Two different techniques were used. In the first, applicable only to τ decays into three or more charged particles, the distance d between the decay vertex and the production vertex was measured. This is related to the lifetime via

$$d = \gamma \cdot \beta \cdot c \cdot t^*,$$

where t^* is the decay time in the tauon rest system and the γ factor is essentially determined by the beam energy $\gamma = E_{\text{beam}}/m_\tau$. The average production vertex position was measured for each filling, using large

I Introduction

The τ lepton, or tauon, is a fundamental particle of the standard model and its lifetime τ_τ is an important

^a Now at LBL, Berkeley, Calif, USA

^b Now at MIT, Cambridge, Mass, USA

^c Now at SLAC, Calif, USA

^d Universität-Gesamthochschule Wuppertal, Wuppertal, FRG

^e Now at Universität des Saarlandes, Saarbrücken, FRG

^f Now at ST Systems Corporation, Lanham, Md, USA

^g Now at MBB, München, FRG

^h Now at DESY, Hamburg, FRG

ⁱ Now at Bayer AG, Brunsbüttel, FRG

^j Now at CALTEC, Calif, USA

^k Now at MPI, Heidelberg, FRG

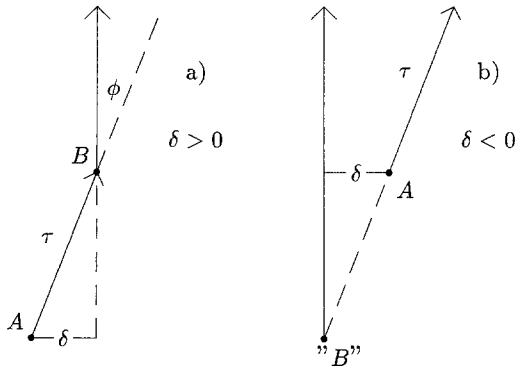


Fig. 1a, b. Definition of the impact parameter δ and its sign. In **a** the tauon is created at point A and decays at point B . The projection onto the $r-\phi$ plane of the tauon and the decay particle trajectory are shown. The impact parameter δ is the distance of closest approach in the $r-\phi$ plane of the observed decay particle trajectory to the production point. Because of measurement errors the "decay point" B can be reconstructed on the wrong side of the production point as sketched in **b**. In this case δ is given a negative sign.

angle $e^+e^- \rightarrow e^+e^-$ scattering. Including radiative effects, the expected $\langle d \rangle / \tau_\tau$ is $2860 \mu\text{m}/\text{ps}$ at $\sqrt{s} = 35 \text{ GeV}$.

In the second method the impact parameter δ is measured. This, as shown in Fig. 1, is the distance of closest approach of a decay particle trajectory to the production vertex. This distance, measured in the $r-\phi$ plane i.e. perpendicular to the beam direction, is given by $|\delta| = t^* |\sin \theta| |\sin \phi| p_\tau / m_\tau$, where θ is the angle between the tauon and the beam directions and ϕ the angle between the tauon direction and that of the decay product, whose impact parameter is being measured. The measurement was restricted to the $r-\phi$ plane since there the measurement accuracy of the detector is best. The sign of δ is defined as shown in Fig. 1. Negative values of δ can occur because of measurement errors or incomplete knowledge of the tauon direction. For the present analysis the relation between $\langle \delta \rangle$ and τ_τ is $161 \mu\text{m}/\text{ps}$. The advantage of the impact parameter method is that also one prong decays, which amount to about 86% of all τ -decays, can be used.

For both the decay length and impact parameter the expected effects of the finite lifetime are similar to or smaller than the experimental uncertainties. It is therefore essential that the resolution functions of the apparatus are well understood or at least well parametrized. This is discussed in some detail in Sect. II after the description of the apparatus. The measurement of the position of the interaction point is presented in Sect. III, the tauon selection in Sect. IV, the analysis in Sect. V, and finally in Sect. VI the results are discussed and compared with other recent measurements of τ_τ .

II Apparatus

The JADE detector is described in [1]. Here we review only the tracking system, which is of special relevance for this analysis and which was improved for this experiment.

In 1984 the JADE-detector was equipped with a vertex chamber which is essentially an extension of the central jet-chamber to smaller radii replacing the former beam pipe counters. It is, as the jet-chamber, azimuthally divided into 24 cells, each vertex chamber cell containing 7 sense wires. The wire planes of the vertex chamber are rotated by half a drift space relative to those of the central jet chamber. The innermost sense wire of 760 mm length is located at a radial distance of 99 mm from the beam line. The distance between two sense wires is 9 mm. The chamber was mounted around an aluminium beam pipe of 180 mm diameter, which had a wall thickness of 3 mm. This relatively large diameter was chosen because the chamber was installed before PETRA had reached its maximum energy and it was feared that a narrow beam pipe could cause serious background problems.

The chamber was operated with a gas mixture of Argon (89.1%), CO_2 (9.9%) and CH_4 (1%) slightly above atmospheric pressure at a constant gas density. The read out was accomplished by Flash-ADC's which measured the signal amplitude at both ends of each wire every 10 nanoseconds with a 6 bit resolution. These data were then analysed within the CAMAC-system by several microprocessors which recorded the shape of all signal pulses. Based on this pulse shape information the drift-time was determined off-line. In the $r-\phi$ plane a spatial resolution for isolated tracks of about $110 \mu\text{m}$ was obtained. The double track resolution was 1.5 mm. No effort was made to determine the z -coordinate, that is the component along the beam direction, using the vertex chamber. The vertex chamber was mechanically connected to the central drift chamber via the beam pipe support system located at about $\pm 1.5 \text{ m}$ from the interaction point.

Most of the data used for the present analysis were taken during 1986, when the central jet chamber was equipped with a fast Flash - ADC - system. For details see [2]. This new readout system improved the spatial resolution of the central jet-chamber from 170 to $110 \mu\text{m}$, and the double pulse resolution from 7 to 2 mm.

The location of the vertex chamber relative to the jet-chamber was determined using Bhabha events. The relative position in the $r-\phi$ plane was determined for every run period with an accuracy of about $\pm 20 \mu\text{m}$. The material between the vertex chamber and the central chamber amounted to 0.10 radiation

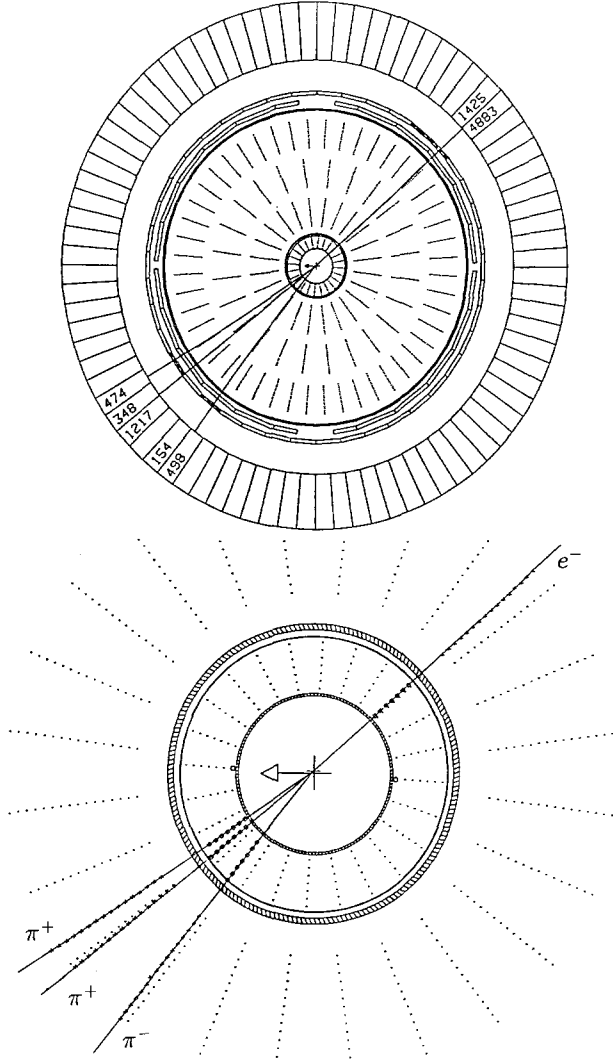


Fig. 2. Illustration of a τ -event showing the tracks of a τ -pair in the central part of the JADE detector. The view is in beam direction showing from the center outwards, the vertex chamber, the jet chamber – an enlarged view of this inner part is shown in b) – and the z-chamber followed by a ring of scintillation counters and the barrel lead glass counters. The τ^- in this event decays into an electron, which deposits an energy of 6.3 GeV in the lead glass, and the τ^+ into 3 charged particles

lengths. In fitting the particle trajectory to the measured space points in both chambers we allowed for scattering in this material. The scattering angle was a free parameter in the fit with an associated error given by the expected amount of multiple scattering.

An illustration of a typical $e^+e^- \rightarrow \tau^+\tau^-$ event in the JADE detector is shown in Fig. 2. In this event the tauon decayed into an electron while its antiparticle decayed into three charged particles. The enlarged view of the central region shows the vertex chamber more clearly.

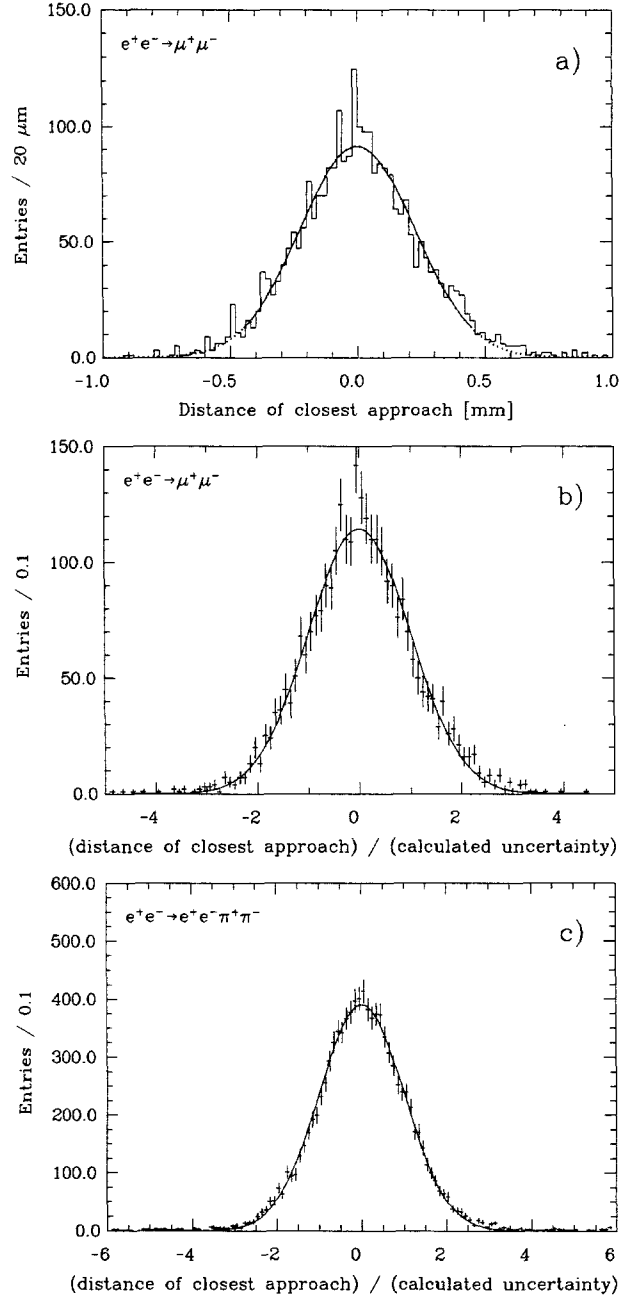


Fig. 3a–c. The distance of closest approach of collinear muon tracks from the reaction $e^+e^- \rightarrow \mu^+\mu^-$ is shown in **a**. The curve shows a fit with a normal distribution yielding $\sigma = 225 \mu\text{m}$. In **b** the distance is divided by its calculated uncertainty (s.d.) for each entry. The curve shows a normal distribution of zero mean and unit variance. In **c** the same distribution as in **b** is shown but for collinear tracks of low momentum from the process $e^+e^- \rightarrow e^+e^-\pi^+\pi^-$

For each track, the uncertainty of its extrapolation to the origin was calculated from the scattering of the individual hits around the fitted track and from the particle momentum and the material traversed by the particle. In order to correctly describe the ob-

served distributions it was found to be necessary to scale the calculated uncertainties by two factors; the first of these, a factor of 1.6, scales the constant part of the vertex resolution and the second, a factor of 1.35, scales the momentum dependent part. In Fig. 3a the measured distance of closest approach of the two muon tracks from the reaction $e^+e^- \rightarrow \mu^+\mu^-$ is plotted. Applying the above scaling factors one expects the distribution shown by the full line in Fig. 3a. This is a normal distribution with $\sigma = 225 \mu\text{m}$, yielding a single track resolution at the interaction point of $160 \mu\text{m}$. In Fig. 3b the distance of closest approach divided by its calculated uncertainty is plotted. The data are well described by a normal distribution with unit variance. In order to demonstrate that the assumed errors are also reasonable for low momentum tracks, we show in Fig. 3c the normalised distance of closest approach of collinear pions with $\langle p_\pi \rangle = 0.5 \text{ GeV}/c$ from the reaction $e^+e^- \rightarrow e^+e^-\pi^+\pi^-$. Here again the data are well described by the same distribution.

III Production point

Both methods of measuring τ_τ require that the position and extension of the luminous region be known. It was assumed that both of these quantities were constant over a given fill and that the shape of the luminous region was constant for a given energy. The mean position of the interaction vertex for each fill, the fill vertex, was determined in the $r-\phi$ plane using a sample of highly collinear Bhabha events, typically about 40 per fill. The fill vertex was defined to be that point at which the sum of the distances of closest approach of the Bhabha tracks to the point was minimal. The positions of the fill vertices are shown in Fig. 4.

Considerable jumps occurred, especially in the x -direction, i.e. in the machine plane, whenever the beams were realigned. The extension of the luminous region transverse to the beam is given in Table 1. The numbers observed are in good agreement with those expected from the machine physics characteristics.

As a check of this procedure we plot in Fig. 5 the distance of closest approach to the fill vertex of tracks from muon pair events. The distance Δ is divided by σ , where σ is the uncertainty on the track extrapolation discussed in the previous section, the extension and the statistical uncertainties in the position of the luminous region. The data are well described by a normal distribution with unit variance indicating that the various contributions to Δ and its variance σ have been accurately determined.

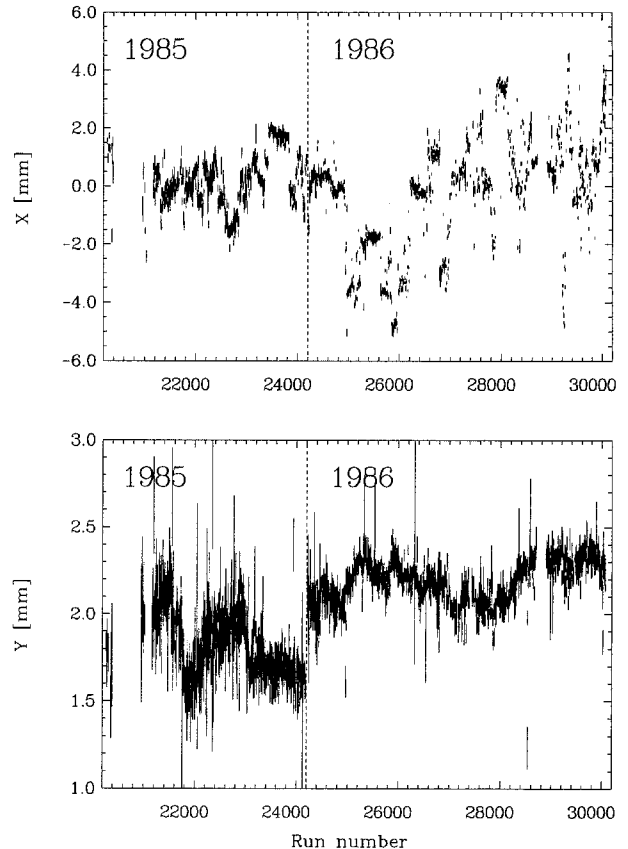


Fig. 4. Distribution of fill vertices for the run period 1985 and 1986. Only runs with active vertex chamber are considered. The $x-y$ coordinates are transverse to the beam direction at the interaction region, x is in the machine plane, y normal to it

Table 1. Parameter list of the 1985 and 1986 data on τ production

Data	1985	1986
$\langle \sqrt{s} \rangle$ [GeV]	41.5	35
Int. luminosity [pb^{-1}]	21.2	85
# of fills	698	1333
Extension of luminous region		
σ_x [μm]	390	330
σ_y [μm]	70	30
# of observed $\tau^+\tau^-$ -pairs	556	2994
# of accepted 3 or more prong decays	110	538
# of accepted one prong decays	–	3132

IV Data

Only data taken while the vertex chamber was active are considered in this analysis. The data were accumulated during 1985 and 1986 and the corresponding integrated luminosities are listed in Table 1. The event selection, described in detail in [3], aimed at a good

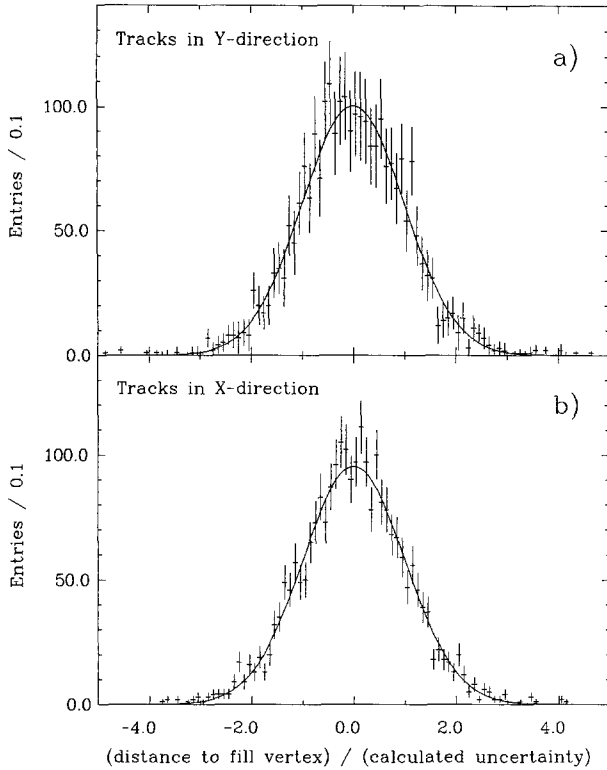


Fig. 5a, b. The distance of closest approach to the fill vertex divided by the calculated uncertainty (s.d.) of muon tracks from the reaction $e^+e^- \rightarrow \mu^+\mu^-$. In **a** tracks close to the vertical, in **b** close to the horizontal direction are plotted. In **a** the average uncertainty is 350 μm , in **b** 220 μm

detection efficiency for all decay modes. Events in which both tauons decay into electrons or both into muons were excluded. The overall detection efficiency for τ -pairs, including the final visual scan, is $(36.6 \pm 1.0)\%$, as determined by Monte Carlo simulation. The resulting number of tauon pairs is given in Table 1.

For the τ decay vertex determination it was required that 3 or 5 tracks be visible in the central drift chamber. Each track, with the possible exception of one, was required to have associated hits in the vertex chamber. Tracks which could have originated from photon conversion in the material of the beam pipe or the tracking chambers were eliminated before these cuts were applied.

The τ decay vertex was determined from these tracks, in the $r-\phi$ plane, by minimizing a properly defined χ^2 -function. The χ^2 -probability distribution P_{χ^2} is constant with the exception of a peak close to 0, which is due to the remaining background from photon conversion and K_s^0 decays. A further cut, $P_{\chi^2} \geq 7\%$, was made in order to obtain a clean sample of τ decays. The remaining background of about 4% is from tauon production by 2-photon collisions

$e^+e^- \rightarrow e^+e^-\tau^+\tau^-$ ($\sim 2\%$), for which the tauon momentum and opening angle distributions differ from the one of the annihilation events, and from hadron production $e^+e^- \rightarrow \text{hadrons}$ ($\sim 2\%$).

Only one prong decays were used for the measurement of the impact parameter. The restriction to one prong decays was in order to have a statistically independent sample. The analysis was restricted to the 1986 data as these were taken at a constant energy. The different energy settings of the 1985 data were not fully simulated in the Monte Carlo calculations. A detailed simulation, however, is essential for the impact parameter method. The one track had to have at least 4 associated hits in the vertex chamber and a momentum exceeding 1 GeV/c. The background in this one prong sample is again estimated to be about 4%. The largest contributions are from the reactions $e^+e^- \rightarrow e^+e^-\tau^+\tau^-$ ($\sim 1.7\%$) and $e^+e^- \rightarrow e^+e^-$ or $\mu^+\mu^-$ ($\sim 1.3\%$).

V Analysis

V.a Vertex method

The decay vertex (x_v, y_v) in the $r-\phi$ plane is determined by minimizing the function

$$\chi^2(x_v, y_v) = \sum_i \frac{\Delta_i^2}{\sigma_i^2},$$

where Δ_i is the distance of closest approach of track i to the vertex in the $r-\phi$ plane, and σ_i the corresponding uncertainty. The $r-\phi$ plane, which is perpendicular to the beam direction, is chosen as it is the plane in which particle's trajectory is most precisely measured. The decay length d is determined from the vector \mathbf{l} between the production and decay vertex and the tauon flight direction. The vector \mathbf{l} is constrained to be parallel to the projection of the flight direction onto the $r-\phi$ plane. The flight direction was approximated by the momentum sum of the charged decay products, to an accuracy of about 2° , which is sufficient for the determination of d .

The distributions of the measured decay lengths and their uncertainties are shown in Fig. 6. The error is dominated by the uncertainty in the decay vertex measurement while the uncertainty in the fill vertex position makes only a small contribution. Also shown in Fig. 6 are the distributions obtained from a Monte Carlo simulation assuming $\tau_\tau = 280$ fs, which describe the data quite well.

The lifetime was determined by a maximum likelihood fit to the d distribution for events within $|d| \leq 10$ mm and $\sigma_d \leq 7.5$ mm. In the fit allowance was

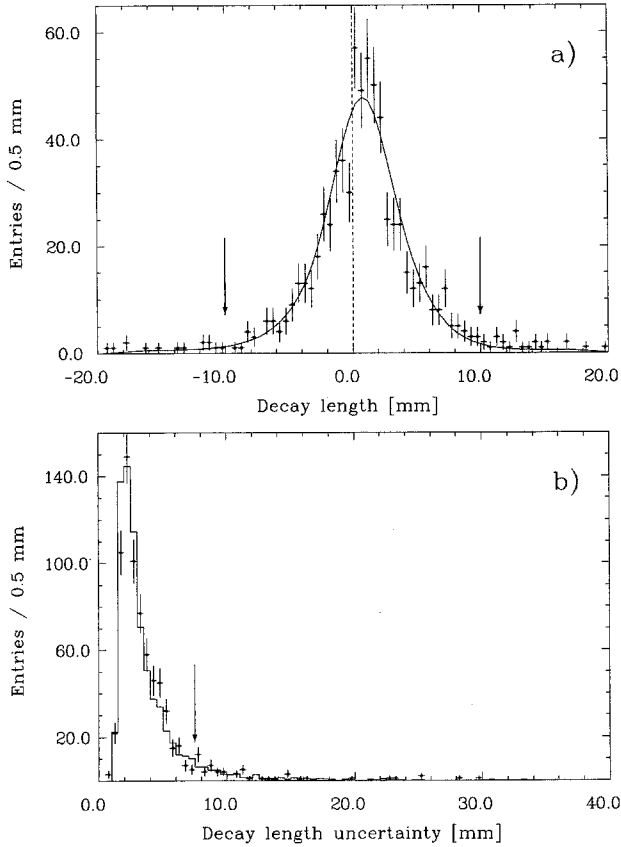


Fig. 6a, b. The distribution of measured decay lengths **a** and of their calculated uncertainties (s.d.) **b**. The curves show the results of a Monte Carlo simulation assuming $\tau_\tau = 280$ fs. The cuts applied are indicated

made for all known background sources which, with the exception of $e^+e^- \rightarrow e^+e^-\tau^+\tau^-$ and the very small contribution from $e^+e^- \rightarrow c\bar{c}$, were assumed to be created at the interaction point.

The straightforward fitting procedure, however, would yield a result which is slightly biased for the following reason. The probability distribution used for the likelihood function is essentially an exponential folded with a gaussian distribution. The width of the latter is primarily determined by the uncertainties in the decay vertex position. This uncertainty increases with decreasing opening angle of the decay products. The scattering in the beam pipe, however, affects the measured opening angle distribution. If it increases the opening angle, then the observed decay length is longer than the true one and the uncertainty attributed to the vertex is smaller. The reverse happens if the opening angle is decreased by the scattering in the beam pipe. This effect causes long decay lengths to have too large a weight. In the fitting procedure a linear correction was applied to compensate for this effect. If we denote by d_0 the “true” decay length

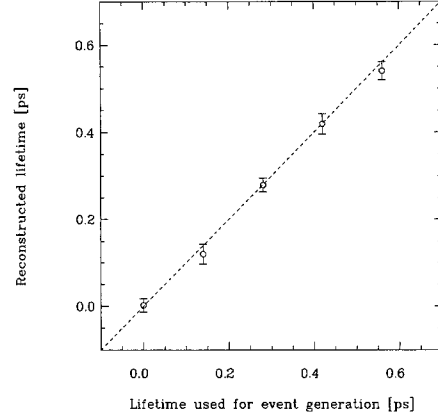


Fig. 7. Generated versus reconstructed values of τ_τ from a Monte Carlo simulation. After application of the correction described in the text the results are consistent with the identity indicated by the diagonal

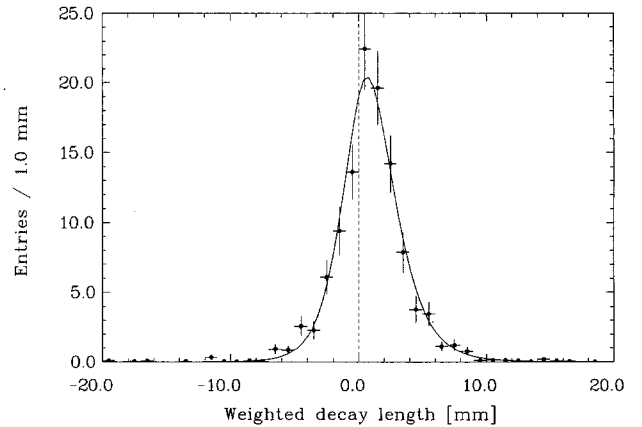


Fig. 8. Decay length distribution weighted by the inverse square of its error (s.d.). The full line represents the best fit curve

and by d its measured value, then

$$\sigma_d(d) = \sigma_d(d_0) + \frac{\partial(\sigma_d)}{\partial d}(d - d_0) + \dots$$

The “true” uncertainty $\sigma_d(d_0)$, which is needed for an unbiased fit, was approximated by replacing d_0 by the expected average \bar{d} and the gradient $\frac{\partial(\sigma_d)}{\partial d}$ was determined from Monte Carlo studies. With this correction the fit yields unbiased results, as is demonstrated with Monte Carlo data in Fig. 7, where the lifetime used in the event generation is plotted versus the one obtained from the fit. Without this correction the line would be shifted upwards by about 50 fs.

Figure 8 shows the distribution of the measured decay lengths weighted by the inverse square of their uncertainties. The result of the maximum likelihood

fit is also shown. The resulting lifetime is $\tau_\tau = \left(309^{+35}_{-34}\right)$ fs, where only statistical errors are given.

The systematic uncertainty is dominated by the uncertainties in the detector resolution and is estimated to be about ± 11 fs. The result obtained by the vertex method is thus

$$\tau_\tau = \left(309^{+35}_{-34} \pm 11\right) \text{ fs.}$$

*V**b** Impact parameter method*

The impact parameter method is considerably more complicated than the decay vertex technique for several interrelated reasons. The observable effects of the tauon lifetime are small and the relation between the impact parameter and the decay time is more involved than the one to one correspondence, ignoring radiative effects, between decay length and decay time. Furthermore, a good knowledge of the tauon flight direction, of the position and shape of the luminous region and of the detector resolution are more critical. These drawbacks are partially compensated by the larger number of one prong decays.

For the one prong decays, used in this analysis, the tauon flight direction could obviously not be deduced from the momentum of the single charged decay product. The tauon direction was therefore approximated by an axis defined in a similar way to the thrust axis. The axis was chosen such that $\sum_i |p_i^\parallel|$

be maximal, where p_i^\parallel was the momentum component along the axis. The sum extends over all observed charged and neutral decay products of both tauons, with the exception of the particle whose impact parameter was to be measured, which was omitted to avoid correlations. It is important that the distribution of this axis be correctly described by the Monte Carlo simulation. Fig. 9 shows a comparison between data and simulation of the particle momenta and of the angle between the axis described above and the particle momentum in the $r-\phi$ plane. The measured impact parameter distribution is shown in Fig. 10 together with Monte Carlo predictions for $\tau_\tau = 0, 280$ and 560 fs. It is evident that a value of $\tau_\tau = 280$ fs describes the data best. It is also evident, however, that the tails of the distribution are not properly described by the simulation. The events in this region were visually inspected and were mostly found to contain a track from a nuclear interaction within the beam pipe or the detector material or a track, which was poorly measured because it traversed the central jet chamber very close to a wire plane. These events

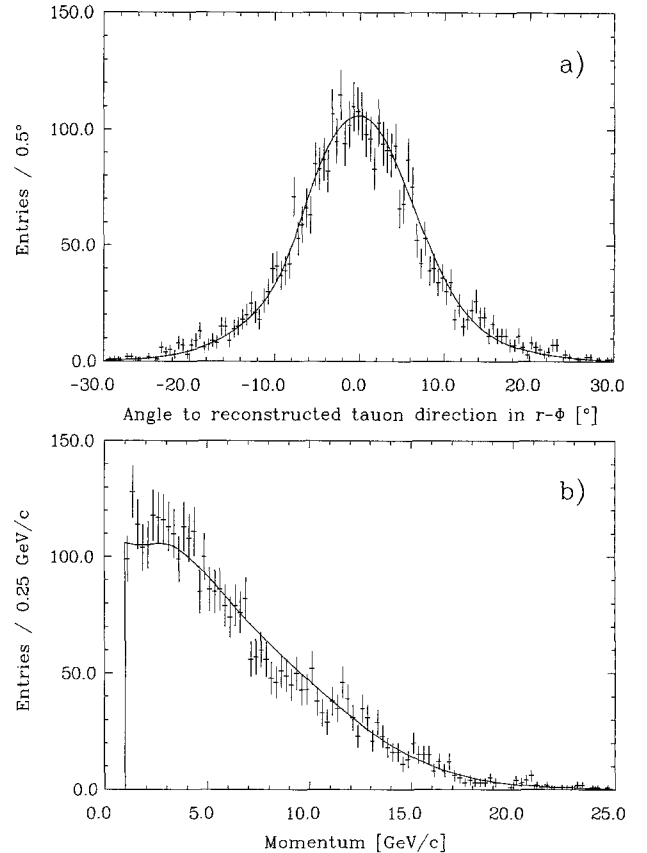


Fig. 9 a b. The distribution of the angle between the reconstructed tauon direction and the direction of the particle used to determine δ is shown in **a**. The full line is the result of the Monte Carlo simulation. The momentum distribution of the decay particles is shown in **b**

amounted to about 1.5% of the event sample. Within errors they are symmetrically distributed around $\langle \delta \rangle$ with a s.d. of ~ 1.7 mm and are taken into account in the fitting procedure by a background term with a gaussian distribution. This term is in addition to the previously mentioned backgrounds which were estimated by Monte Carlo techniques.

The weighted impact parameter distribution together with the best fit curve is shown in Fig. 11. The mean central value of the distribution is $(51 \pm 6) \mu\text{m}$ and its variance $\sigma_\delta = 350 \mu\text{m}$. From a maximum likelihood fit we obtain $\tau_\tau = (289 \pm 33)$ fs.

The systematic uncertainties of the impact parameter technique are considerably larger than those of the decay length determination. We estimate a systematic error of 26 fs. The main contributions are the uncertainties in the detector resolution (~ 20 fs), the location of the interaction region (~ 11 fs), and in the background at large $|\delta|$ (~ 8 fs). We estimate a systematic uncertainty in the fill vertex of $40 \mu\text{m}$ in both directions. The statistical uncertainties of the fill ver-

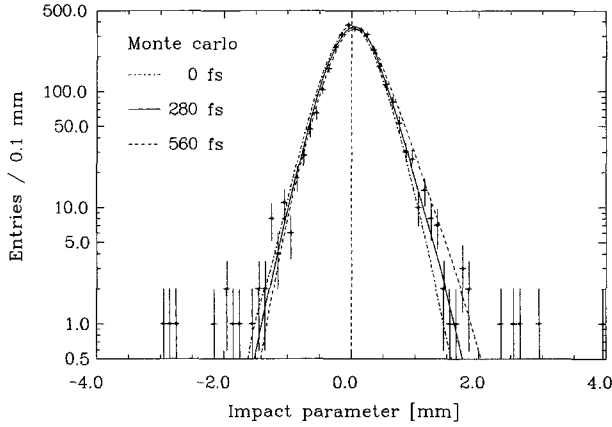


Fig. 10. Impact parameter distribution together with Monte Carlo prediction for 3 different values of τ_τ

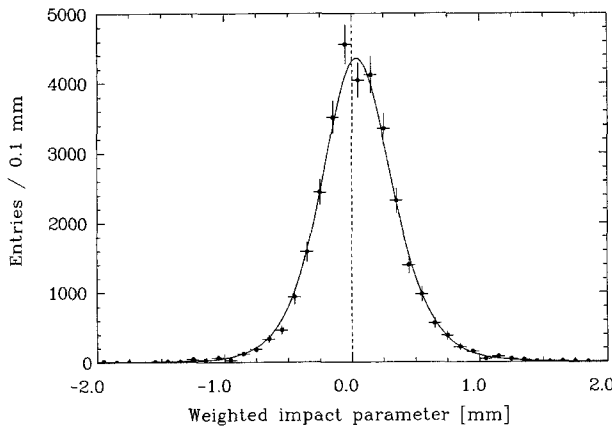


Fig. 11. The distribution of the impact parameter weighted by the inverse square of its uncertainty (s.d.). The full line shows the best fit to the data

tex which are indicated in Fig. 4 are taken into account in the fitting procedure and are contained in the statistical error of τ_τ .

The final result obtained using the impact parameter technique is

$$\tau_\tau = (289 \pm 33 \pm 26) \text{ fs.}$$

VI Summary and conclusion

The two measurements of τ_τ are in good agreement. We therefore combine the two results, weighting them by the inverse of the quadratic sum of the statistical and systematic uncertainties. The statistical uncertainties of the two measurements are uncorrelated since the τ decay samples are independent. The partial correlation of the systematic uncertainties is taken into account. The resulting average which we quote

Table 2. Compilation of recent accurate measurements of the tauon decay time τ_τ

τ_τ [fs]	Reference
295 ± 18	ARGUS 87 [4]
325 ± 23	CLEO 87 [5]
302 ± 17	HRS 87 [6]
309 ± 19	MAC 87 [7]
288 ± 23	MARK II 87 [8]
306 ± 24	TASSO 88 [9]
301 ± 29	this experiment

Table 3. Leptonic decay branching fractions of the tauon

$B(\tau \rightarrow e \bar{\nu}_e \nu_\tau)$	0.170 ± 0.011	JADE	[10]
$B(\tau \rightarrow e \bar{\nu}_e \nu_\tau)$	0.173 ± 0.005	world average	[11]
$B(\tau \rightarrow \mu \bar{\nu}_\mu \nu_\tau)$	1.010 ± 0.040	world average	[11]
$B(\tau \rightarrow e \bar{\nu}_e \nu_\tau)$			
$B(\tau \rightarrow \mu \bar{\nu}_\mu \nu_\tau)$	0.973	theory	
$B(\tau \rightarrow e \bar{\nu}_e \nu_\tau)$			

as our final result is

$$\tau_\tau = (301 \pm 29) \text{ fs,}$$

where the error includes statistical and systematic uncertainties.

A compilation of recent precise measurements of τ_τ is given in Table 2, where the statistical and systematic errors of each experiment have been added in quadrature. The agreement between the various experiments is good. The weighted average of all measurements is (303 ± 8) fs.

For a check of lepton universality according to (1) the electronic decay fractions of the tauon have to be known. A recent measurement of $B(\tau \rightarrow e \bar{\nu}_e \nu_\tau)$ by JADE as well as the world average value are listed in Table 3. Taking the JADE results only we obtain $G_\tau/G_\mu = 0.95 \pm 0.06$, a ratio in good agreement with universality $G_\tau = G_\mu$. Using the world average values of τ_τ and $B(\tau \rightarrow e \bar{\nu}_e \nu_\tau)$ one obtains $G_\tau/G_\mu = 0.954 \pm 0.020$. The deviation from τ - μ universality, however, diminishes if electron-muon universality is assumed and the measurements of $B(\tau \rightarrow \mu \bar{\nu}_\mu \nu_\tau)$ are included for the determination of $B(\tau \rightarrow e \bar{\nu}_e \nu_\tau)$. This is obvious from the numbers given in Table 3.

Clearly a considerable reduction of the individual measurement errors of both τ_τ and $B(\tau \rightarrow e \bar{\nu}_e \nu_\tau)$ is needed before a violation of τ - μ universality can be claimed from such a deviation; and the present situation is best summarized by stating $G_\tau = G_\mu$ within 8% at 95% C.L. It may nevertheless be worthwhile to remind the reader that measurements [12] of the

axial vector coupling constants via the angular symmetries in the reactions $e^+e^- \rightarrow \tau^+\tau^-, \mu^+\mu^-$ also yield, with a significance of about 2 s.d., somewhat lower values for the tauon than for the muon.

References

1. JADE-Coll. W. Bartel et al.: Phys. Lett. 88 B (1979) 171
2. G. Eckerlin et al.: IEEE Trans. Nucl. Sci. NS-34, 1 (1987) 182
3. JADE-Coll. W. Bartel et al.: Phys. Lett. 161 B (1985) 188
4. ARGUS-Coll. H. Albrecht et al.: Phys. Lett. 199 B (1987) 690
5. CLEO-Coll. C. Bebek et al.: Phys. Rev. D 36 (1987) 2519
6. HRS-Coll. M. Abachi et al.: Phys. Rev. Lett. 59 (1987) 2519
7. MAC-Coll. H.R. Band et al.: Phys. Rev. Lett. 59 (1987) 415
8. MARK II-Coll. D. Amidei et al.: Phys. Rev. D 37 (1988) 1750
9. TASSO-Coll. W. Braunschweig et al.: DESY 88-034, 1988
10. JADE-Coll. W. Bartel et al.: Phys. Lett. 182 B (1986) 216
11. D. Hitlin: in Proceeding of the 1987 International Symposium on Lepton and Photon Interactions at High Energies, Hamburg 1987, p. 217, W. Bartel, R. Rückl, (eds.), Amsterdam; North Holland
12. R. Felst: in Proceeding of "Physics in Collisions 7" Tsukuba, Japan, 1987, T. Kondo, K. Takahashi, (eds.), Singapore: World Scientific